Supplementary Information (SI) for Journal of Materials Chemistry A.

Supporting Information

Tailoring Platinum Content in High-Entropy PdAuMoWPt Alloy for Efficient and Durable Hydrogen Evolution across broad pH Range

Liyi Pan[1], Qian Wang[1], Dongmei Huang[1], Xinhang Ma[1], Yao Qin[1], Qian Sun[1,2], Peng Xie[1,2], Shuangliang Zhao[1,2], Zengxi Wei[1,2*]

[1]University Engineering Research Center of Green Chemical New Materials, School of Chemistry and Chemical Engineering, Guangxi University, Nanning, Guangxi 530004, PR. China.

[2]State Key Laboratory of Featured Metal Materials and Life-cycle Safety for Composite Structures, Guangxi University, Nanning 530004, China

*To whom correspondence should be addressed. E-mails: zengxiwei@gxu.edu.cn

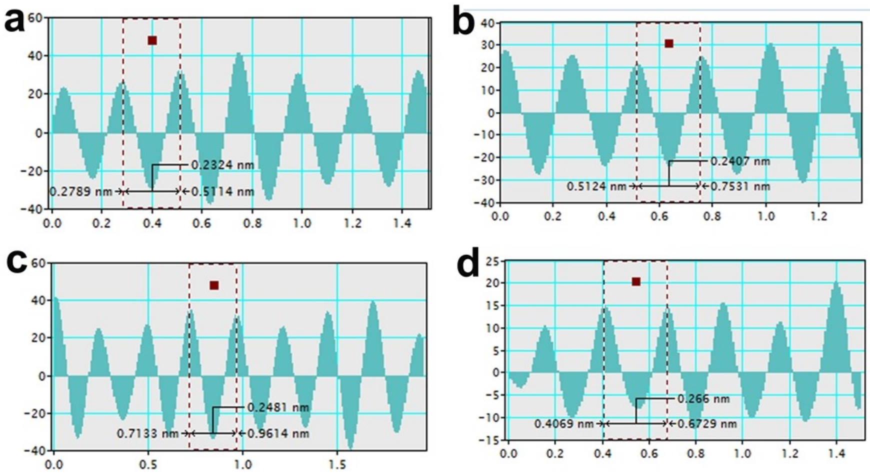

Figure S1. (a–d) Interplanar spacing: (a) HEA-4, (b) HEA -13, (c) HEA -19, and (d) HEA-28

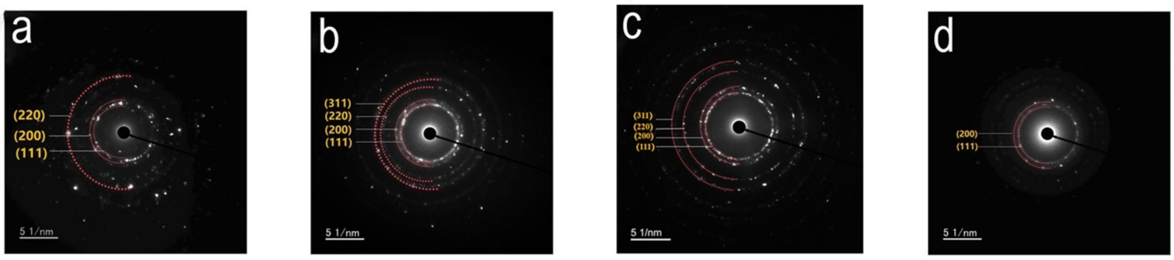

Figure S2. (a–d) Selected-area electron diffraction (SAED) patterns: (a) HEA-4, (b) HEA -13, (c) HEA -19, and (d) HEA-28.

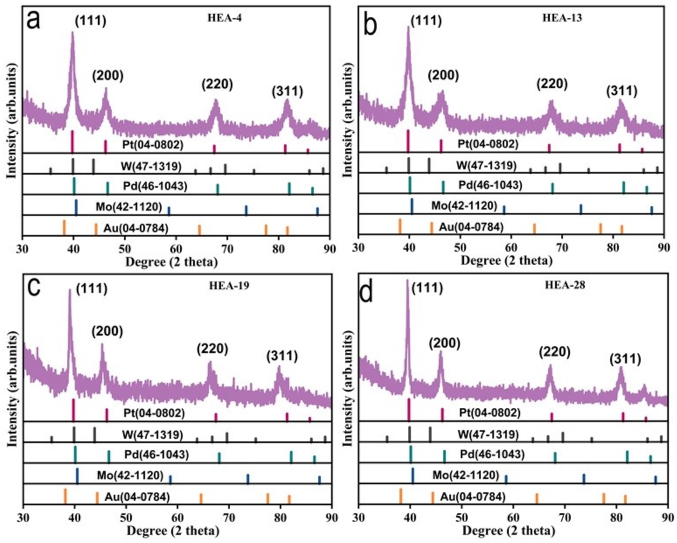

Figure S3.X-ray diffraction (XRD) patterns of PdAuMoWPt HEAs with different Pt contents: (a) HEA-4, (b) HEA-13, (c) HEA-19, and (d) HEA-28.

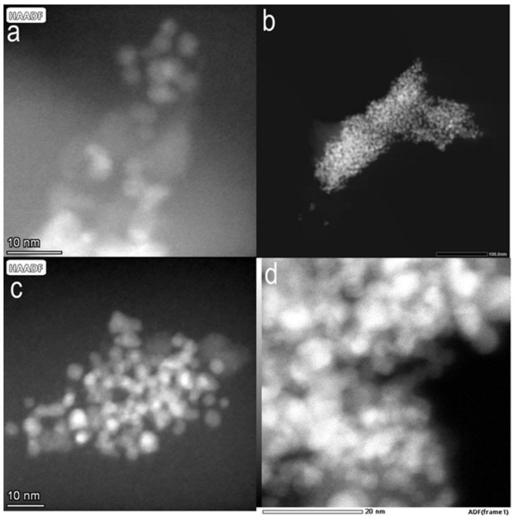

Figure S4.HAADF-STEM images of PdAuMoWPt HEAs with different Pt contents: (a) HEA-19, (b) HEA-13, (c) HEA-4, and (d) HEA-28.

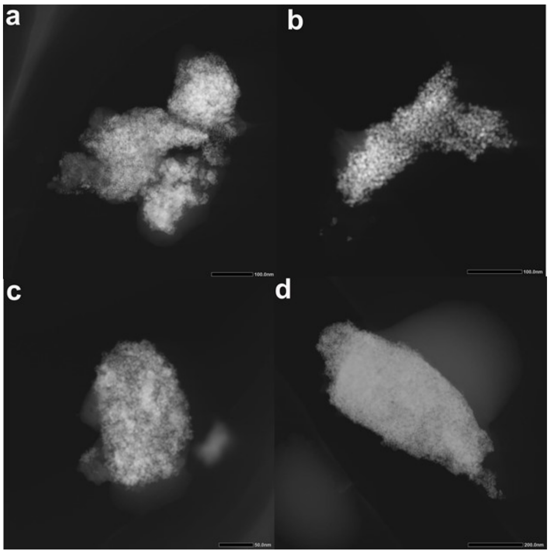

Figure S5. HAADF-STEM images of PdAuMoWPt HEAs with different Pt contents: (a) HEA-4, (b) HEA-13, (c) HEA-19, and (d) HEA-28.

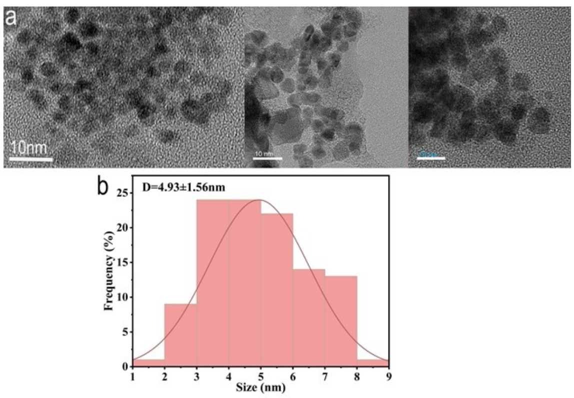

Figure S6. HRTEM image: (a) HEA-28，Particle size distribution histograms and Gaussian fitting curves for HEA-28.

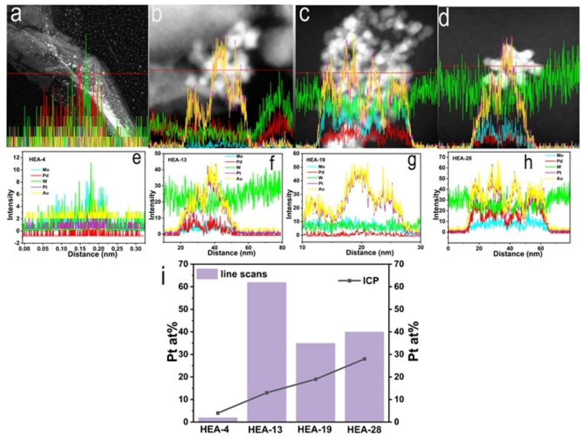

Figure S7. (a–h) EDS line scan profiles of Pd, Au, Mo, W, and Pt elements for HEA-4 (a e), HEA-13 (b f), HEA-19 (c g), and HEA-28 (d h), respectively. (i) Comparison of Pt atomic percentages obtained from EDS line scans and ICP analysis for the four HEAs.

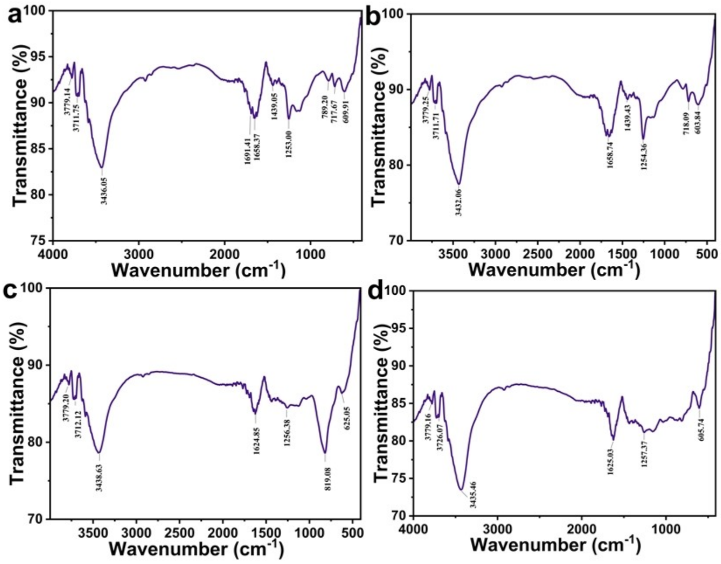

Figure S8. FTIR spectra of PdAuMoWPt HEAs: (a) HEA-4, (b) HEA-13, (c) HEA-19, and (d) HEA-28.

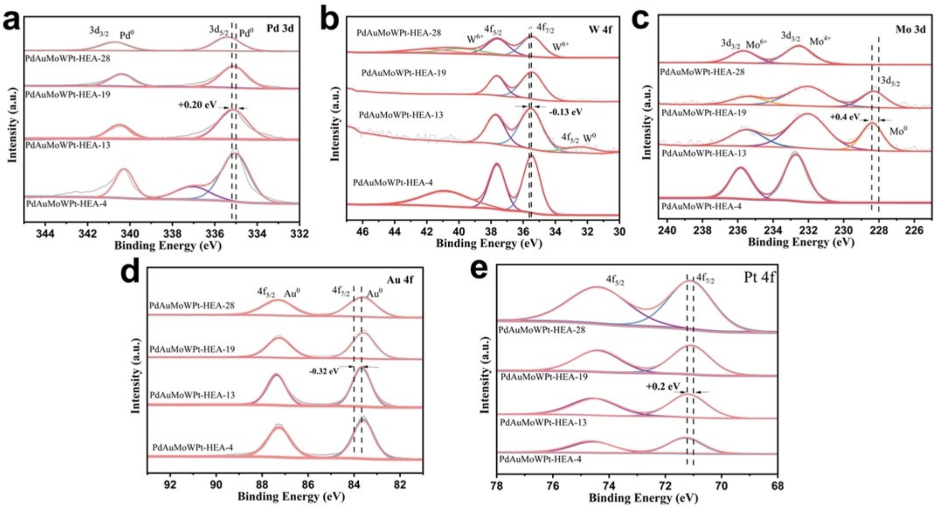

Figure S9. XPS spectra of (a) Pd 3d, (b)W 4f, (c) Mo 3d, (d) Au 4f, (e) Pt 4f of HEA-4, HEA -13, HEA -19, and HEA-28.

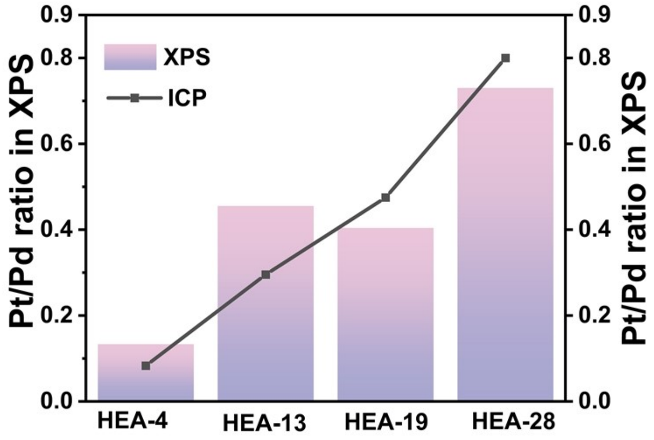

Figure S10. Comparison of Pt/Pd ratios determined by XPS (surface composition) and ICP-MS (bulk composition) for HEA-4, HEA-13, HEA-19, and HEA-28.

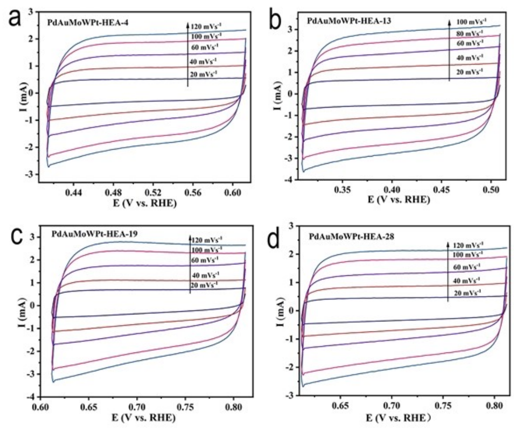

Figure S11. Typical CVs of the samples with scanning rates ranging from 20 to 120 mV/s of (a) PdAuMoWPt HEA-4, (b) PdAuMoWPt HEA-13, (c) PdAuMoWPt HEA-19, (d) PdAuMoWPt HEA-28. The scanning potential range is from 0.30 V to 0.85 V (vs. RHE) in 0.5 M H_2SO_4 solution.

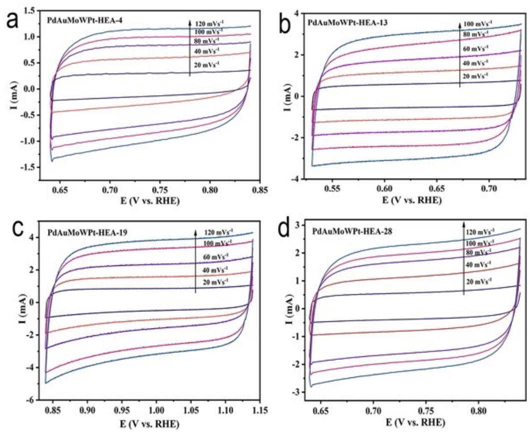

Figure S12. Typical CVs of the samples with scanning rates ranging from 20 to 120 mV/s of (a) PdAuMoWPt HEA-4, (b) PdAuMoWPt HEA-13, (c) PdAuMoWPt HEA-19, (d) PdAuMoWPt HEA-28. The scanning potential range is from 0.53 V to 1.15 V (vs. RHE) in 1 M KOH solution.

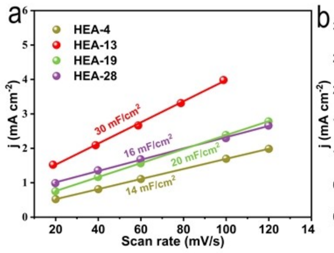

Figure S13. The estimation of Cdl by plotting the capacitive current density against the scan rate to fit a linear regression of PdAuMoWPt HEA. (a) 0.5M H_2SO_4 (b) 1 M KOH.

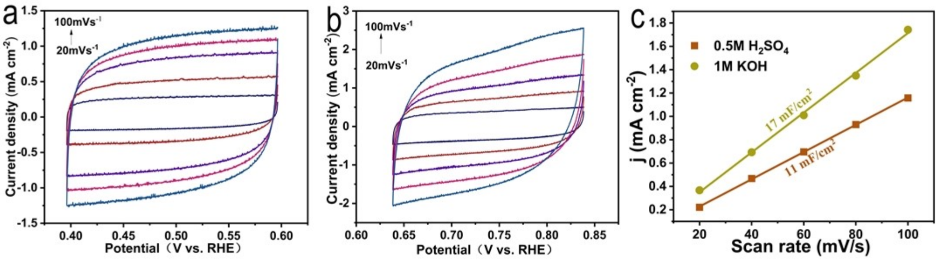

Figure S14. Typical CVs of the samples with scanning rates ranging from 20 to 100 mV/s of Pt (a) H_2SO_4 and (b) 1M KOH, The estimation of Cdl by plotting the capacitive current density against the scan rate to fit a linear regression of commercial Pt/C (C).

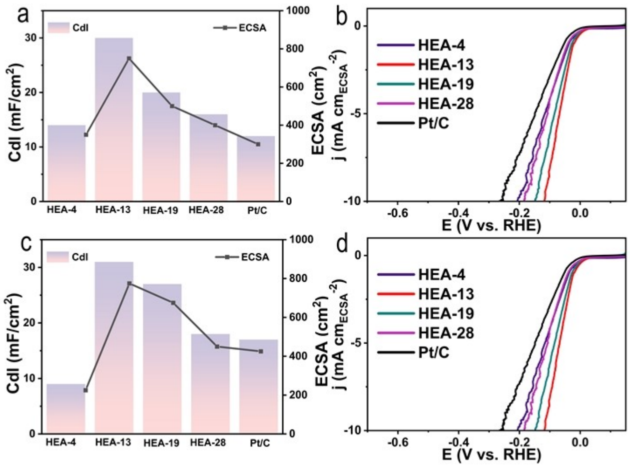

Figure S15：Electrochemical surface area (ECSA) analysis of PdAuMoWPt HEAs and commercial Pt/C. (a, c) Double-layer capacitance (Cdl) and derived ECSA values for HEA-4, HEA-13, HEA-19, HEA-28, and Pt/C in (a) 0.5 M H_2SO_4 and (c) 1 M KOH. (b, d) ECSA-normalized polarization curves of the same catalysts under (b) acidic and (d) alkaline conditions

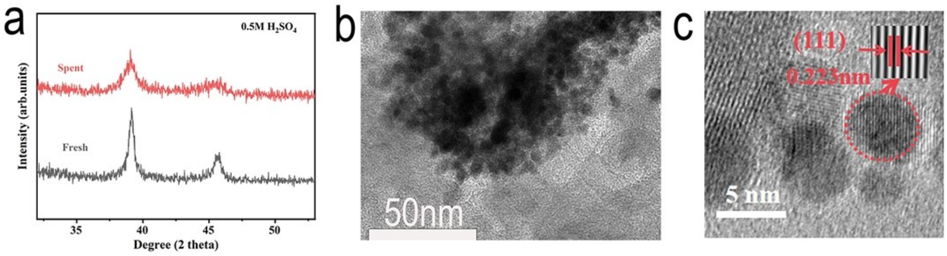

Figure S16. (a) XRD, (b) TEM, (c) HRTEM of PdAuMoWPt HEA -13 after long term stability test in 0.5 M H_2SO_4 solution.

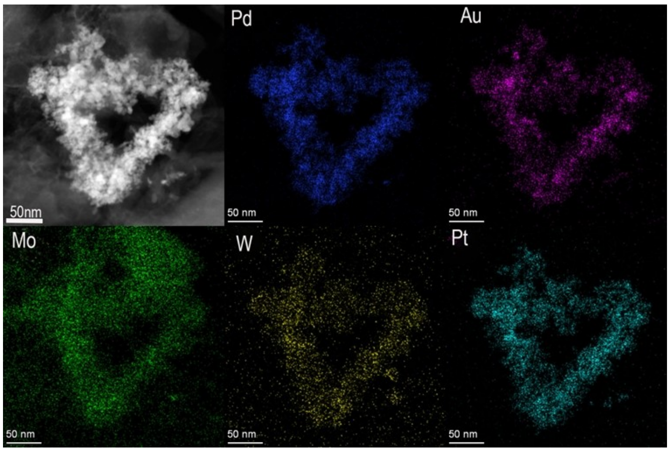

Figure S17. STEM-EDS mapping images of the spent sample after the stability test.

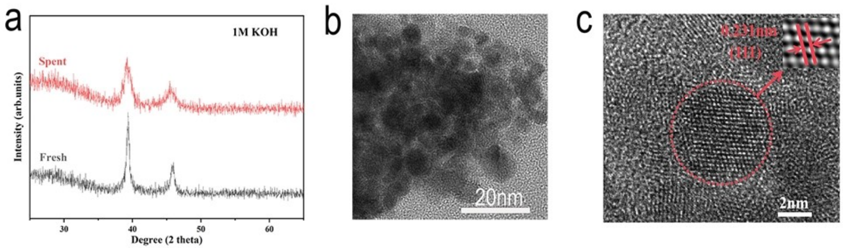

Figure S18. (a) XRD, (b) TEM, (c) HRTEM patterns of PdAuMoWPt HEA-13 after long term stability test in 1M KOH solution.

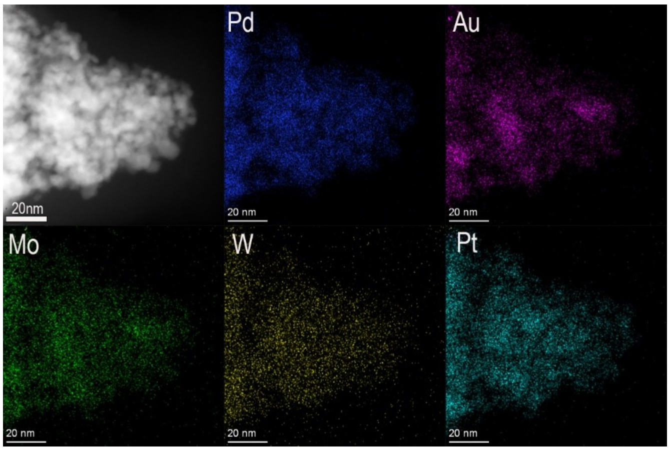

Figure S19. STEM-EDS mapping images of the spent sample after the stability test in 1 M KOH.

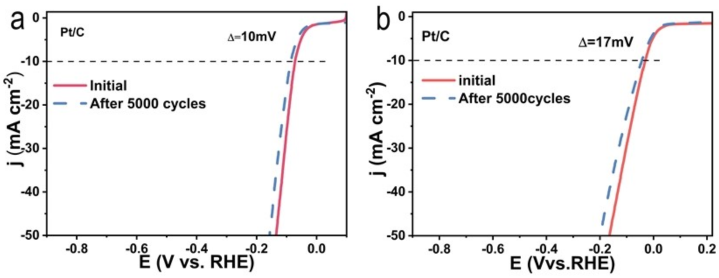

Figure S20. LSV curves of Pt/C before and after accelerated degradation tests (ADT) for only 5000 CV cycles in 0.5 M H2SO4 solution (a) and 1M KOH solution (b).

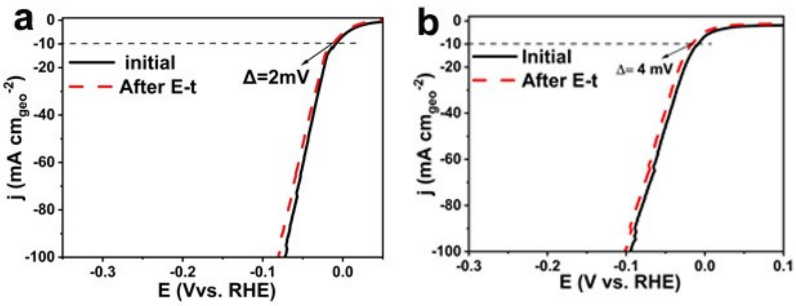

Figure S21. LSV curves before and after the stability test. (a) 0.5M H_2SO_4 , (b) 1 M KOH.

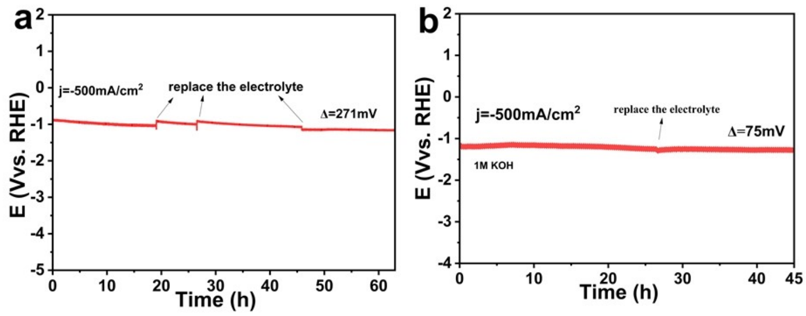

Figure S22. Long-term stability test of HEA-13 at −500 mA,(a) 0.5M H_2SO_4 , (b) 1 M KOH.

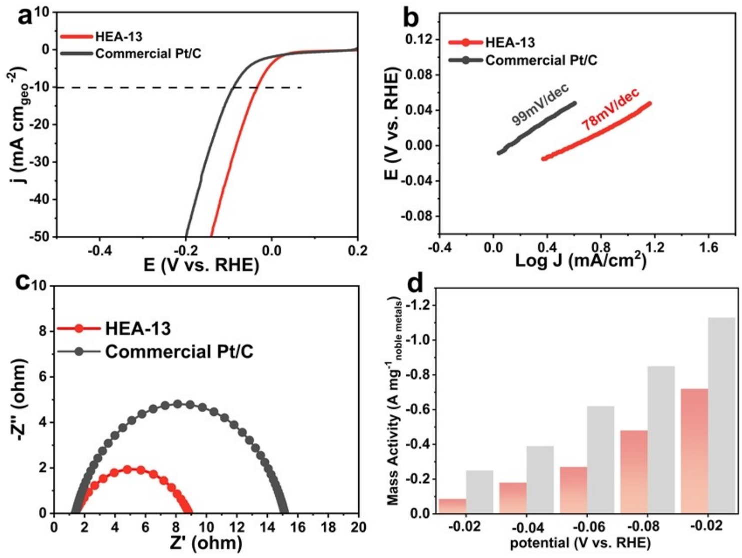

Figure S23. Electrocatalytic HER performance of HEA-13 compared with commercial Pt/C in neutral electrolyte (0.5 M phosphate buffer solution, pH ≈ 7). (a) Linear sweep voltammetry (LSV) curves. (b) Corresponding Tafel plots. (c) Electrochemical impedance spectroscopy (EIS) Nyquist plots at −0.05 V vs. RHE. (d) Mass activity comparison at different overpotentials, normalized to the mass of noble metals.

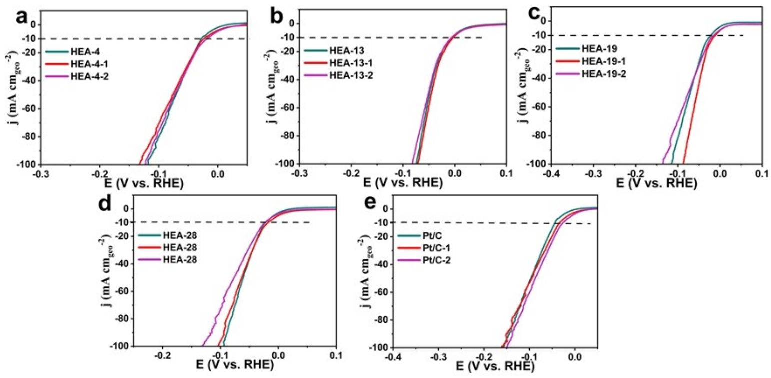

Figure S24. Polarization curves of (a) HEA-4, (b) HEA-13, (c) HEA-19, (d) HEA-28, and (e) commercial Pt/C catalysts, each measured three times under identical conditions to demonstrate reproducibility in H2SO4.

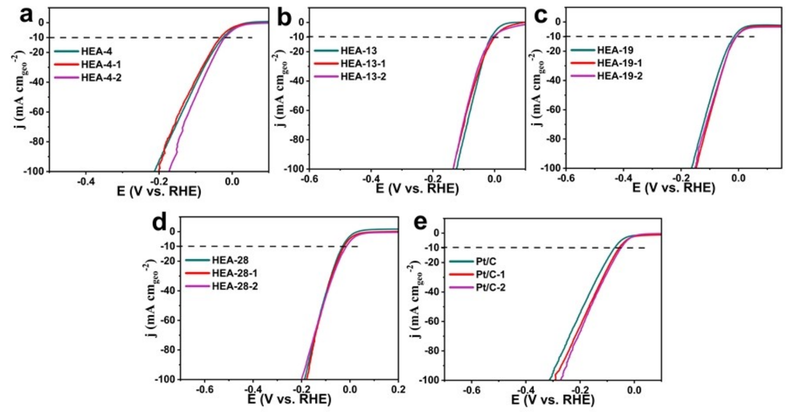

Figure S25. Polarization curves of (a) HEA-4, (b) HEA-13, (c) HEA-19, (d) HEA-28, and (e) commercial Pt/C catalysts, each measured three times under identical conditions to demonstrate reproducibility in KOH.

Table S1. The ICP analysis of the PdAuMoWPt HEA. The units are atomic percentages (atom%).

Element	Atom%			
Pt	4	13	19	28
Pd	48	44	40	36
Au	23	21	20	17
Mo	14	13	13	12
W	11	9	8	7

Table S2. ICP-MS analysis of the electrolyte after durability tests of PdAuMoWPt HEAs.

Analytes	Electrolyte concentration (g/L)	Average concentration (mg/L)	Electrolyte
Mo	0.1134	0.283382875	H_2SO_4
Mo	0.1160	0.28997345	H_2SO_4
Mo	0.1149	0.28721075	H_2SO_4
Mo	0.4469	1.117225625	KOH
Mo	0.4507	1.1267068	KOH
Mo	0.4459	1.114873075	KOH
Pd	0.2317	0.579147875	H_2SO_4
Pd	0.2166	0.541556225	H_2SO_4
Pd	0.2370	0.5925274	H_2SO_4
Pd	0.0971	0.242786425	KOH
Pd	0.0944	0.235881875	KOH
Pd	0.0958	0.2394061	KOH
W	0.1626	0.406452	H_2SO_4
W	0.1786	0.4465294	H_2SO_4
W	0.1741	0.435289325	H_2SO_4
W	0.4743	1.1856422	KOH
W	0.4759	1.18982675	KOH
W	0.4694	1.173416175	KOH
Pt	0.2581	0.645268575	H_2SO_4
Pt	0.2697	0.6742857	H_2SO_4
Pt	0.2647	0.66182945	H_2SO_4

Pt	0.0924	0.2310893	KOH
Pt	0.0980	0.2450322	KOH
Pt	0.0961	0.2402998	KOH
Au	0.2523	0.6307032	H_2SO_4
Au	0.2685	0.671350825	H_2SO_4
Au	0.2603	0.6508296	H_2SO_4
Au	0.1380	0.34497735	KOH
Au	0.1510	0.37761195	KOH
Au	0.1508	0.377064875	KOH

Table S3. The electrochemical impedance spectra fitting results of PdAuMoWPt HEA-13. (Rs: solution resistance; Rct: charge transfer resistance).

Electrolyte	Parameter	Pt/C	PdAu MoW Pt-HEA-4	PdAu MoW Pt-HEA-13	PdAu MoW Pt-HEA-19	PdAu MoW Pt-HEA-28
0.5 M H_2SO_4	Rs	1.4	1.4	1.6	1.3	1.5
	Rct	1	1.4	0.7	1.1	2
1.0 M KOH	Rs	2	1.5	2.5	2.5	2.5
	Rct	5.3	17.5	2.7	3.9	7

Table S4. Comparison of the overpotential at 10 mA cm^{-2} and Tafel slope of advanced HEA catalysts reported in the recent literatures for H ER in 0.5M H_2SO_4 electrolyte.

Catalysts	**Overpotentia(mV vs. RHE)**	**Tafel Slope (mV dec^{-1})**	**Ref.**
PdAuMoWPt	7.13	52	This work
NiCoFePtRh	27	30.1	J. Am. Chem. Soc.,2021 143 (41)
PdMoGaInNi	13	127.6	ACS Catal., 2022 12(19): 11955-11959.
IrPdPtRhRu	12	30.1	Nano Mater. Sci., 2024.
PtFeCoNiCu	12	28.1	Nat. Commun., 2024, 15(1): 359
CoFeNiPtTa	10.6	37	ACS Appl. Nano Mater., 2022, 5(7): 9810-9817.
Ru-PtFeNiCuW	9	19.2	Adv. Mater., 2023, 2400433.
RhRuPtPdIr	30	31	J. Mater. Chem. A, 2024, 12(10): 5668-5678.
PtRuCoNiCu	19	/	Nano Res., 2024: 1-7.
FeCoNiMnW	15	34	Chem. Eng. J., 2022, 446: 137452.
PtCoNiRuIr	18	34.2	Small Methods, 2024, 18(4): 2948-2957.
PdPtCuNiP	32	44.6	Adv. Funct. Mater., 2021, 31, 38,2101586
NiCoFePtRh	27	30.1	J. Am. Chem. Soc., 2019, 143, 41, 17117-17127
IrPdPtRhRu	17	/	Chem. Sci., 2020, 47, 12731- 12736
NiCo-SAD-NC	55	31.5	Nat. Commun., 2021, 12, 6766
Ru/OMSNNC	27	/	Adv. Mater., 2021, 33, 12, 2006965
Ru@Ni-MOF	37	33	ANGEW. CHEM. INT. ED., 2021, 60, 41, 22276-22282
PtRu/mCNTs	28	22.6	Energy Environ. Sci., 2022,15,102-108
Pt3Co@NCNT	42	27.2	ANGEW. CHEM. INT. ED., 2021, 60, 35, 19068-19073
PtSi	22	33	Adv. Energy Mater., 2022, 12, 20, 2200293
MI-PtZnCo	20	25.4	Adv. Energy Mater., 2022, 12, 2201478

Table S5. Comparison of the overpotential at -10 mA cm^{-2} and Tafel slope of advanced HEA catalysts reported in the recent literatures for HER in 1 M KOH electrolyte.

Catalysts	**Overpotentia(mV vs. RHE)**	**Tafel Slope (mV dec^{-1})**	**Ref.**
PdAuMoWPt	6.53	66	This work
IrPdPtRhRu	16	31	Nano Mater. Sci.，2024
PdPtRhIrCu	15	37	Adv. Funct. Mater., 2023,33(42): 2 304963.
Ru-PtFeNiCuW	16	27.9	Adv. Mater.,2400433.
PtFeCoNiCuCr	29	136.42	Adv. Funct. Mater.
PtPdRhRuCu	23.3	124	Adv. Funct. Mater., 2024: 2414554 .
FeCoNiCuTiGa	47	35.75	ACS Appl. Energ. Mater.，2024
PtRhNiFeCu	13	29.8	Small, 2024:2309819.
FeCoNiCuTi	64.9	36.81	Chem. Eng. J., 2024, 492: 152145.
PtIrNiCoFe	14	16.9	Adv. Mater., 2024: 2304867.
FeCoNiCuA$_{l2}$ Mn	9.7	56.9	Small Methods, 2024: 2301691.
RhRuPtPdIr	65	78	J. Mater. Chem. A, 2024, 12(10): 5 668-5678.
FeCoNiCuPtIr @CNT	21	54.5	Adv. Funct. Mater., 2022,32,19,31 2110645
FeCoNiCuPd	29	47.2	ENVIRON., 2022, 313, 15, 12147 2
T-Pt-Co4N	31	35	ACS Nano, 2022, 16, 11, 18038-18047
FeCoPdIrPt@GO	42	82	Nat. Commun., 2020, 11, 2016
FeCoNiAlTi	88.2	40.1	Adv. Mater., 2020, 32, 21, 2000385
PtNi-O/C	40	79	J. Am. Chem. Soc 2018, 140, 29, 9046 –9050
NiCo-SAD-NC	61	55	Nat. Commun., 2021, 12, 6766
Pt3Co@NCNT	36	34.8	ED., 2021, 60, 35, 19068- 19073
AgNi-5 NCs	24	61	ED., 2020, 59, 7, 2881- 2889
PtSi	38	47	Adv. Energy Mater., 2022, 12, 20, 2200293
MI-PtZnCo	29	64.2	Adv. Energy Mater., 2022, 12, 2201478
Ptx@Niy-rGO	37	43	Nano Res., 2022, 15, 965- 971
N-PdIr	34	81.9	J. Mater. Chem. A, 2022,10, 8364-8370
PtNi	42	85	J. Am. Chem. Soc. 2018, 140, 29, 9046–9050

References

1. Y. Yao, Z. Huang, L. A. Hughes, J. Gao, T. Li, D. Morris, S. E. Zeltmann, B. H. Savitzky, C. Ophus, Y. Z. Finfrock, Q. Dong, M. Jiao, Y. Mao, M. Chi, P. Zhang, J. Li, A. M. Minor, R. Shahbazian-Yassar and L. Hu, *Matter*, 2021, **4**, 2340-2353.
2. B. Hammer and J. K. Nørskov, in *Adv. Catal.*, Academic Press, 2000, vol. 45, pp. 71-129.
3. Y.-Y. Ma, C.-X. Wu, X.-J. Feng, H.-Q. Tan, L.-K. Yan, Y. Liu, Z.-H. Kang, E.-B. Wang and Y.-G. Li, *Energy Environ. Sci*, 2017, **10**, 788-798.
4. D. H. Kweon, M. S. Okyay, S.-J. Kim, J.-P. Jeon, H.-J. Noh, N. Park, J. Mahmood and J.-B. Baek, *Nat. Commun*, 2020, **11**, 1278.
5. C. Wang, J. Zhang, K. Miao, M. Long, S. Lai, S. Zhao and X. Kang, Adv. Mater, 2024, **36**, 2400433.
6. M. Wei, Y. Sun, J. Zhang, F. Ai, S. Xi and J. Wang, *Energy Environ. Sci*, 2023, **16**, 4009-4019.